Electronic Supporting Information

Design and Synthesis of Photoluminescent Active Interpenetrating Metal–Organic Frameworks Using N-2-Aryl-1,2,3-Triazole Ligands

Jingyang Li[a], Ying He[b], Li Wang[a], Qinhe Pan[c], Zhiguang Song*[a] and Xiaodong Shi*[b]

a. State key Laboratory of Supramolecular Structure and Materials, College of Chemistry, Jilin University, Changchun, Jilin13002 China; E-mail szg@jlu.edu.cn
b. Department of Chemistry, University of South Florida, 4202 E. Fowler Avenue, Tampa, Florida 33620, United States. E-mail: xmshi@usf.edu
c. Key Laboratory of Advanced Materials of Tropical Island Resources
Hainan University, Haikou 570228, P. R. China.

1. General Methods and Materials

All commercial reagents and solvents used during synthesizing ligands and MOFs were directly purchased from Energy Chemical, Bidepharm and Heowns without further purification. Single crystal X-ray diffraction data were obtained from Siemens Smart CCD diffractometer with graphite-monochromated Mo Ka (λ = 0.71073 Å) radiation at 50 kV and 1.2 mA[1]. Powder X-ray diffraction (PXRD) characterizations were processed by Rigaku D/MAX 2550 diffractometer using CuKa radiation at 40 kV and 200 mA. Fourier transform infrared spectroscopy (FT-IR) measurements were carried out by Bruker. Themal gravimetric analyzer (TGA) results were utilized with TA Instrument, TGA Q500 from room temperature to 800 °C. Elemental analysis of carbon, nitrogen and hydrogen (C, H, and N) results were collected from Elementar vario Micro elemental analyzer. Gas adsorption (N_2 and CO_2) were accomplished by ASAP 2020. Fluorescence observations including excitation, emission spectra and quantum yield were completed by Edinburgh Instrument, FLS 920. Nuclear magnetic resonance (NMR) (^{1}H NMR and ^{13}C NMR) spectra were retrieved from a 400 MHz Bruker Avance NEO. At the same time, chemical shifts were analyzed based on internal tetramethylsilane (δ 0.00 ppm) and $CDCl_3$ (δ 7.26 ppm, δ 1.50 ppm) or DMSO (δ 2.50 ppm, δ 3.30 ppm) for ^{1}H data and $CDCl_3$ (δ 77.00 ppm), DMSO (δ 40.00 ppm) for ^{13}C results. HRMS values were summarized by Brucker ESI APCI. Further purification such as column chromatography was performed on 300-400 mesh silica gel.

2. Synthesis of ligands

2.1 General synthetic procedures

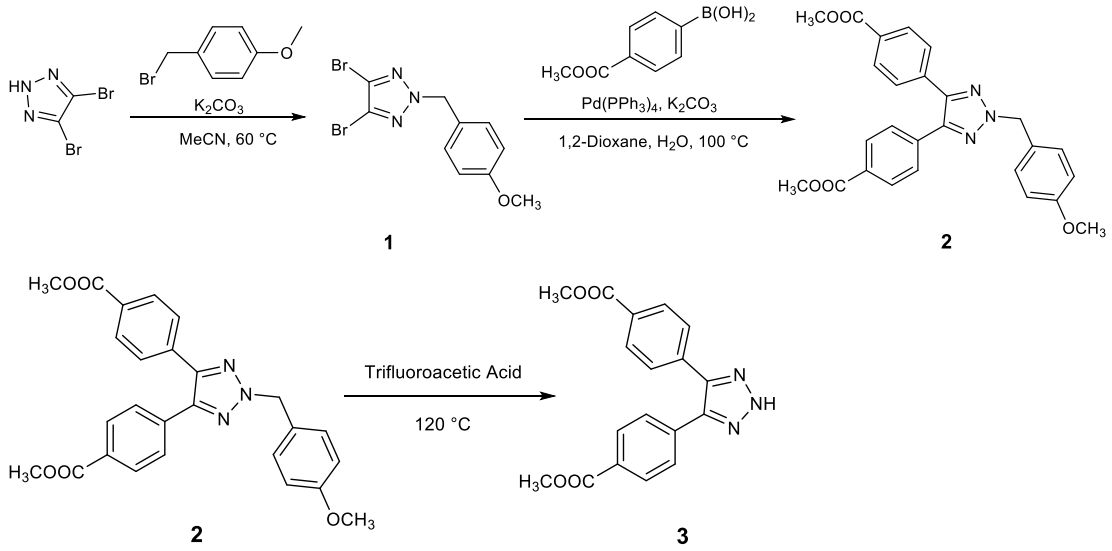

4,5-dibromo-2-(4-methoxybenzyl)-2H-1,2,3-triazole (1)

Mixture of 4,5-dibromo-2H-1,2,3-triazole (5 g, 22 mmol) and potassium carbonated (12.18 g, 88.16 mmol, 4 equiv.) in MeCN was previously stirred about 30 min before injecting 4-Methoxybenzyl bromide (4.87 mg, 24.22 mmol, 1.1 equiv.) slowly under N_2 at room temperature, and kept stirring at 60 ^oC for 72 h followed by TLC. After starting molecule converted completely, the reaction mixture was extracted with ethyl acetate and brine for three times. Then, solvent was concentrated under vacuum and product was further purified by silica gel column chromatography (DCM:PE = 1:1) as white solid (yield 98%).

^{1}H NMR (400 MHz, $CDCl_3$) δ 7.31 (d, *J* = 8.7 Hz, 2H), 6.88 (d, *J* = 8.7 Hz, 2H), 5.44 (s, 2H), 3.80 (s, 3H).

^{13}C NMR (101 MHz, $CDCl_3$) δ 159.98, 129.94, 125.91, 124.56, 114.24, 59.77, 55.26.

HRMS (ESI) m/z calcd. for $[C25H35N5O5Si+H]^+$ 345.9112 found 345.3049.

Dimethyl 4,4'-(2-(4-methoxybenzyl)-2H-1,2,3-triazole-4,5-diyl)dibenzoate (2)

1 (5 g, 14.41 mmol), tetrakis(triphenylphosphine)palladium (0.83 g, 0.72 mmol, 0.05 equiv.), 4-(Methoxycarbonyl)benzeneboronic Acid (7.78 g, 43.23 mmol, 3 equiv.) and potassium carbonate (7.97 g, 57.64 mmol, 4 equiv.) were added into a 100 ml Schlenk tube and degassed three times at room temperature. 1,4-dioxane and deionized water (1:1) were eventually poured into tube and increase reaction temperature to 100 ^oC after repeat degas process. After 12 h, the reaction mixture was extracted with EA and saturated brine and evaporate solvent under vacuum. The mixture was finally purified by silica column chromatography (DCM:EA = 40:1) to obtain white solid product (yield 97%).

^{1}H NMR (400 MHz, $CDCl_3$) δ 8.02 (d, *J* = 8.3 Hz, 1H), 7.60 (d, *J* = 8.4 Hz, 1H), 7.41 (d, *J* = 8.6 Hz, 1H), 6.90 (d, *J* = 8.6 Hz, 1H), 5.59 (s, 1H), 3.92 (s, 2H), 3.79 (s, 1H). **^{13}C NMR** (101 MHz, $CDCl_3$) δ 166.61, 159.76, 144.12, 135.20, 129.86, 128.17, 126.87, 114.16, 58.57, 55.23, 52.14.

HRMS (ESI) m/z calcd. for $[C25H35N5O5Si+H]^+$ 458.1638 found 458.1722.

Dimethyl 4,4'-(2H-1,2,3-triazole-4,5-diyl)dibenzoate (3)

2 (5 g, 10.93 mmol) was dissolved in concentrated trifluoroacetic acid (20 ml) at 120 ^oC for 72 h. Saturated sodium bicarbonate was used to wash excessed TFA until PH = 5. Brine and EA were subsequently utilized to extract mixture. The organic phase was concentrated under vacuum and purified through silica column chromatography (DCM:EA = 20:1) as white solid (54% yield).

^{1}H NMR (400 MHz, $CDCl_3$) δ 8.07 (d, *J* = 8.2 Hz, 1H), 7.63 (d, *J* = 8.2 Hz, 1H), 3.94 (s, 2H).

^{13}C NMR (101 MHz, DMSO) δ 166.76, 138.28, 130.11, 128.69, 128.34, 52.76. **HRMS (ESI)** m/z calcd. for $[C_{25}H_{35}N_5O_5Si+H]^+$ 338.1063 found 338.1160.

2.2 Synthesis of 4,4'-(2-phenyl-2H-1,2,3-triazole-4,5-diyl)dibenzoic acid (L1)

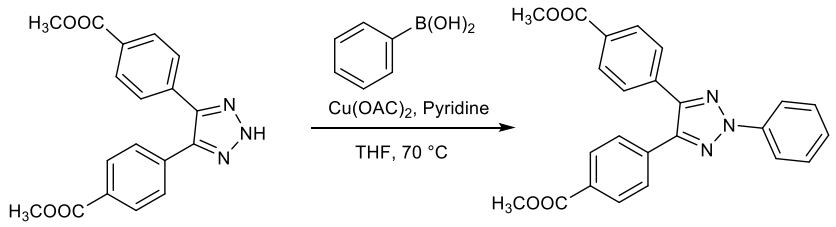

3 4

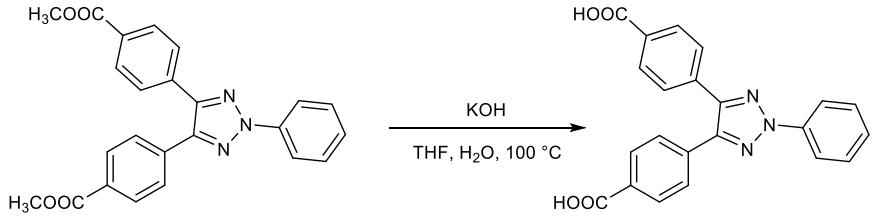

4 L1

Dimethyl 4,4'-(2-phenyl-2H-1,2,3-triazole-4,5-diyl) dibenzoate (4)

3 (1 g, 2.96 mmol), phenylboronic Acid (0.54 g, 4.45 mmol, 1.5 equiv.), $Cu(OA_c)_2$ (0.81 g, 4.45 mmol, 1.5 equiv.) and pyridine (0.47 g, 5.93 mmol, 2 equiv.) were dissolved in anhydrous THF under 1 atm O_2 at 70 °C. After 12 h, the organic solvent was directly purified under vacuum without any extractions and purified by silica column chromatography (DCM:EA = 40:1) as white solid with 50 % yield.

^{1}H NMR (400 MHz, $CDCl_3$) δ 8.19 (d, *J* = 7.7 Hz, 1H), 8.08 (d, *J* = 8.4 Hz, 2H), 7.71 (d, *J* = 8.4 Hz, 2H), 7.53 (t, *J* = 7.9 Hz, 1H), 7.40 (t, *J* = 7.4 Hz, 1H), 3.95 (s, 3H).

^{13}C NMR (101 MHz, $CDCl_3$) δ 166.61, 145.27, 139.43, 134.87, 130.34, 129.95, 129.35, 128.34, 127.92, 118.90, 52.24.

HRMS (ESI) m/z calcd. for $[C_{25}H_{35}N_5O_5Si+H]^+$ 414.1376 found 414.1454.

4,4'-(2-phenyl-2H-1,2,3-triazole-4,5-diyl) dibenzoic acid (L1)

4 (1 g, 2.42 mmol) and potassium hydroxide (1.36 g, 24.2 mmol, 10 equiv.) were dissolved in THF at 100 °C overnight. The organic phase was washed with DCM and water first. In addition, water phase was acidified with concentrated HCl to PH = 1. The white precipitate was then washed again with deionized water and filter under vacuum to collect white solid (yield 98%).

^{1}H NMR (400 MHz, DMSO) δ 13.14 (s, 1H), 8.15 (d, *J* = 7.8 Hz, 1H), 8.04 (d, *J* = 8.3 Hz, 2H), 7.73 (d, J = 8.3 Hz, 2H), 7.64 (t, *J* = 7.9 Hz, 1H), 7.50 (t, *J* = 7.4 Hz, 1H).

^{13}C NMR (101 MHz, DMSO) δ 167.37, 145.59, 139.27, 134.41, 131.68, 130.35, 128.84, 119.14.

HRMS (ESI) m/z calcd. for $[C_{25}H_{35}N_5O_5Si+H]^+$ 386.1063 found 386.1145.

2.3 Synthesis of 4,4',4"-(2H-1,2,3-triazole-2,4,5-triyl)tribenzoic acid (L2)

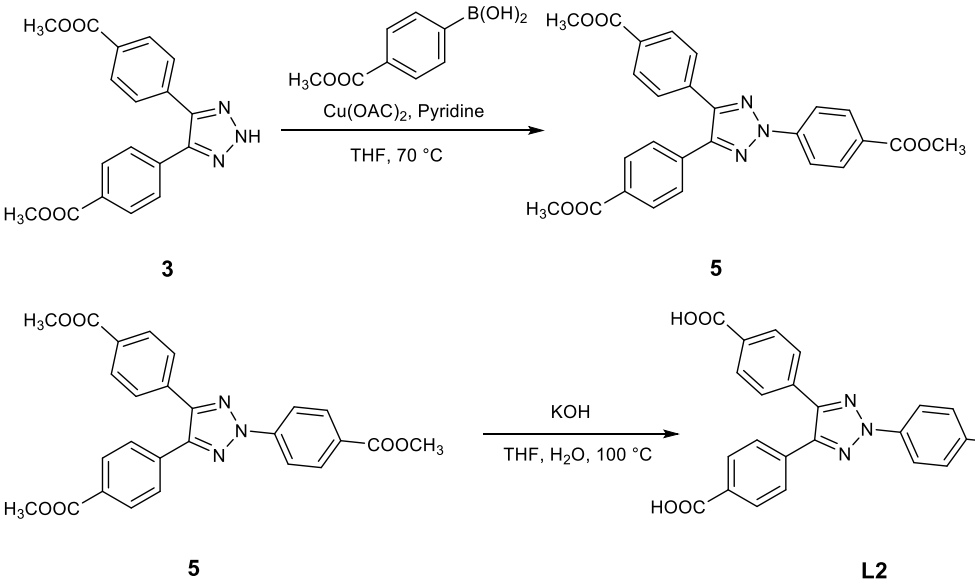

Trimethyl 4,4',4''-(2H-1,2,3-triazole-2,4,5-triyl)tribenzoate (5)

3 (1 g, 2.96 mmol), 4-(Methoxycarbonyl)benzeneboronic Acid (0.80 g, 4.44 mmol, 1.5 equiv.), $Cu(OA_c)_2$ (0.81 g, 4.45 mmol, 1.5 equiv.) and pyridine (0.47 g, 5.93 mmol, 2 equiv.) were dissolved in anhydrous THF under 1 atm O_2 at 70 °C. After 12 h, the organic solvent was directly purified under vacuum without any extractions and purified by silica column chromatography (DCM:EA = 40:1) as white solid with 45 % yield.

^{1}H NMR (400 MHz, $CDCl_3$) δ 8.27 (d, *J* = 9.0 Hz, 1H), 8.22 – 8.17 (m, 1H), 8.09 (d, *J* = 8.5 Hz, 2H), 7.71 (d, *J* = 8.5 Hz, 2H), 3.96 (d, *J* = 3.7 Hz, 4H).

^{13}C NMR (101 MHz, $CDCl_3$) δ 166.49, 166.16, 146.07, 142.29, 134.40, 131.00, 130.59, 129.97, 129.25, 128.36, 118.41, 52.27.

HRMS (ESI)m/z calcd. for $[C_{25}H_{35}N_5O_5Si+H]^+$ 472.1430 found 472.1512.

4,4',4''-(2H-1,2,3-triazole-2,4,5-triyl)tribenzoic acid (L2)

L2 (1 g, 2.12 mmol) was obtained from hydrolysis of **5** with potassium hydroxide (1.19 g, 21.2 mmol, 10 equiv.) in THF at 100 °C overnight. The organic phase was washed with DCM and water subsequently. In addition, water phase was acidified with concentrated HCl to PH=1. The white precipitate was then washed again with deionized water and filter under vacuum to collect white solid (yield 98%).

^{1}H NMR (400 MHz, DMSO) δ 13.19 (s, 1H), 8.27 (d, J = 8.8 Hz, 1H), 8.18 (d, J = 8.8 Hz, 1H), 8.05 (d, *J* = 8.3 Hz, 1H), 7.73 (d, *J* = 8.4 Hz, 1H).

^{13}C NMR (101 MHz, DMSO) δ 167.34, 166.98, 146.29, 141.93, 134.09, 131.88, 131.64, 130.63, 130.35, 128.89, 118.87.

HRMS (ESI) m/z calcd. for $[C_{25}H_{35}N_5O_5Si+H]^+$ 430.096 found 430.9141.

3. MOF synthesis and characterizations

3.1 Synthesis of NAT-MOF-1

The mixture of **L1** (4,4'-(2-phenyl-2H-1,2,3-triazole-4,5-diyl) dibenzoic acid) (20 mg, 0.052 mmol) and $Zn(NO_3)_2{\cdot}6H_2O$ (31 mg, 0.104 mmol) in DMF (3 ml), MeOH (3 ml) and HNO_3 (0.6 ml, 2.2 ml HNO_3 in 10 ml DMF) were transferred into 10 ml glass vial and kept the reaction at 85 ^oC for three days. Obviously, colorless crystals were obtained with 67 % yield (C: 56.90 % H: 4.34 % N: 11.18 %). Characterizations including single crystal data, PXRD plots, FT-IR and TGA curves spectra were illustrated below, respectively. (Table S1, Figure S1(a), Figure S2 (a) and Figure S3(a))

3.2 Synthesis of NAT-MOF-2

L2 (4,4',4''-(2H-1,2,3-triazole-2,4,5-triyl)tribenzoic acid) (20 mg, 0.05 mmol) and $Zn(NO_3)_2{\cdot}6H_2O$ (28 mg, 0.094 mmol) were dissolved in DMF and deionized water (v/v = 3:1) in 10 ml glass vial at 85 ^oC for three days. There were needle-like transparent crystals at the bottom of vial with 63 % yield. Elemental analysis of C was 50.31 %, H was 4.40 % and N was 10.11 %, respectively. Single crystal data, TGA and PXRD spectra were shown in Table S2 Figure S1(b) and Figure S3(b). FT-IR results between **L2** and **NAT-MOF-2** were also characterized in Figure S2(b).

3.3 Single crystal X-ray crystallography for NAT-MOFs

The crystallographic data for **NAT-MOF-1** and **NAT-MOF-2** were collected on a Siemens Smart CCD diffractometer with graphite-monochromated Mo Ka (λ = 0.71073 Å) radiation at a temperature of 299(2) K and 278(2) K, respectively. The structure was solved by direct methods with SHELXT[1] and refined by full-matrix least-squares on F^2 using the SHELXTL-2014[2]. All non-hydrogen atoms were refined with anisotropic displacement parameters. The hydrogen atoms of the ligands were generated geometrically. All structures were examined using the Addsym subroutine of the PLATON software[3] to assure that no additional symmetry could be applied to the models. The contribution of the electron density associated with disordered solvent molecules was removed by the SQUEEZE[4] routine in PLATON. The final formula was derived from crystallographic data combined with elemental and thermogravimetric analyses data. For **NAT-MOF-1**, the disordered C1 atom was refined by ISOR restraint. For **NAT-MOF-2**, the disordered O3, O36, O25, O35, O10, O16 and C103 atoms were refined by ISOR restraint and the Uij values of the displacement parameters for the disordered C and O atoms of coordinated solvent molecules were restrained by SIMU instruction.

1. G.M. Sheldrick, Acta Cryst. (2015). A71, 3–8.

2. G.M. Sheldrick, Acta Cryst. (2015). C71, 3–8.
3. A.L. Spek, J. Appl. Crystallogr. 36 (2003) 7.
4. A.L. Spek, Acta Cryst. (2015). C71, 9–18.

Table S1 Crystal data and structure refinement for NAT-MOF-1.

CCDC number	1974069
Empirical formula	$C_{23}H_{16}N_3O_5Zn$·1.6DMF
Formula weight	479.76
Temperature/K	299(2)
Crystal system	orthorhombic
Space group	C m C a
a/Å	24.0057(12)
b/Å	24.6946(13)
c/Å	8.5544(4)
α/°	90
β/°	90
γ/°	90
Volume/Å^3	5071.1(4)
Z	8
ρ_{calc}g/cm^3	1.257
F(000)	1960
Crystal size/mm^3	0.12 × 0.12 × 0.1
Radiation	MoKα (λ = 0.71073)
2θ range for data collection/°	2.897 to 25.049
Index ranges	-27 ≤ h ≤ 28, -25 ≤ k ≤ 29, -10 ≤ l ≤ 10
Reflections collected / unique	14815/2298 [R_{int} = 0.0322]
Data/restraints/parameters	2298/6/155
Goodness-of-fit on F^2	1.224
Final R indexes [I>=2σ (I)]	R_1 = 0.0433, wR_2 = 0.1403
Final R indexes [all data]	R_1 = 0.0484, wR_2 = 0.1427
Largest diff. peak/hole / e Å^{-3}	0.382/-0.303

Table S2 Crystal data and structure refinement for NAT-MOF-2.

CCDC Number	1974068
Empirical formula	$C_{101}H_{69}N_{15}O_{36}Zn_7$·43.6$H_2O$
Formula weight	2526.30
Temperature/K	278(2)
Crystal system	monoclinic
Space group	P 21 / C

a/Å	29.6681(15)
b/Å	27.6756(17)
c/Å	14.3832(7)
α/°	90
β/°	92.371(2)
γ/°	90
Volume/Å^3	11799.7(11)
Z	4
ρ_{calc}g/cm^3	1.422
F(000)	5112
Crystal size/mm^3	0.1× 0.1 × 0.1
Radiation	MoKα (λ = 0.71073)
2θ range for data collection/°	2.312 to 25.000
Index ranges	-35 ≤ h ≤ 34, -26 ≤ k ≤ 32, -15 ≤ l ≤ 17
Reflections collected / unique	66423 / 19915 [R_{int} = 0.0921]
Data/restraints/parameters	19915/2412/1436
Goodness-of-fit on F^2	1.089
Final R indexes [I>=2σ (I)]	R_1 = 0.0935, wR_2 = 0.2412
Final R indexes [all data]	R_1 = 0.1539, wR_2 = 0.2665
Largest diff. peak/hole / e Å^{-3}	1.850/-1.634

3.4 Powder X-ray diffraction

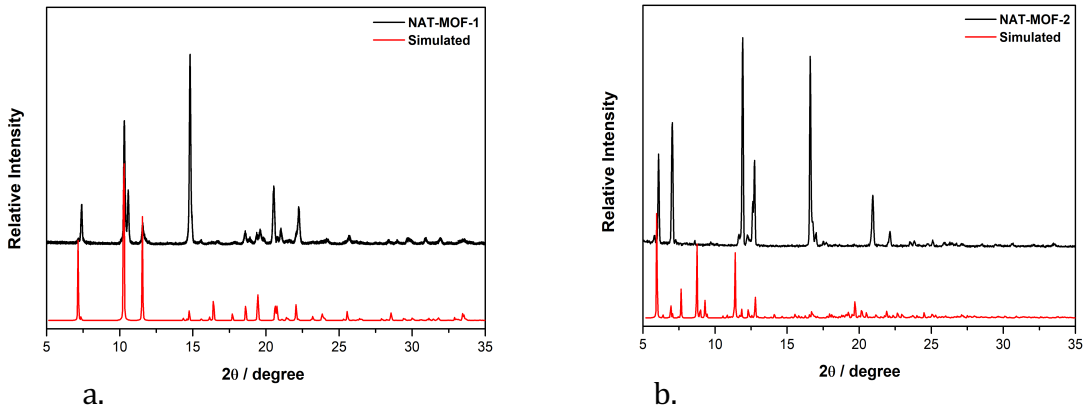

a. b.

Figure S1. PXRD curves of (a) **NAT-MOF-1** and (b) **NAT-MOF-2**

Powder X-ray diffraction (PXRD) characterizations were processed using CuKa radiation at 40 kV and 200 mA from 4° to 35° at room temperature. Figure S1 demonstrates PXRD curves of NAT-MOFs. **NAT-MOF-1** and **NAT-MOF-2** are in good agreement with simulated PXRD that address the successful synthesis of frameworks.

3.5 Fourier transform infrared spectroscopy

Fourier transform infrared spectroscopy (FT-IR) spectra of TADA (**L1**), **NAT-MOF-1**, TATA (**L2**) and **NAT-MOF-2** were tested subsequently. For **L1** and **NAT-MOF-1** (Figure S2a), carboxylic acid groups around 2998 cm^{-1} disappeared while the symmetric and asymmetric stretching of carboxylate groups at 1414 cm^{-1} and 1529 cm^{-1} arise on the contrary. For **L2** and **NAT-MOF-2** (Figure S2b), the FT-IR spectra showed the characteristic band of coordinated carboxylate groups at 1377 cm^{-1} and 1606 cm^{-1} and the disappearance of broad band at 2991 cm^{-1} for carboxylic acid stretching indicates the binding with metal cations.

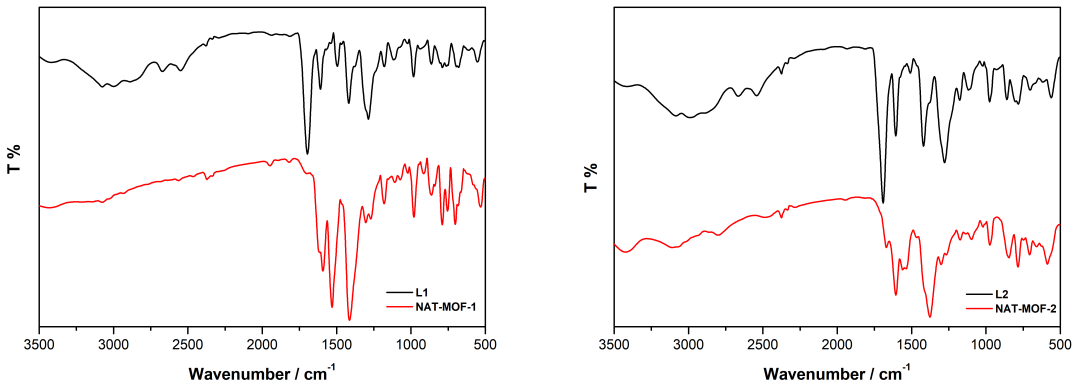

a. b.

Figure S2. FT-IR spectra of (a) **NAT-MOF-1** and (b)**NAT-MOF-2**

3.6 Thermalgravimetric analysis

Thermogravimetric analysis (TGA) were processed from room temperature to 800 ℃ in the air. As-synthesized and activated NAT-MOFs were conducted at the same time (Figure S3). For as-synthesized **NAT-MOF-1** (Figure S3a, black curve), the first weight loss of 15.5 % between 86 ℃ and 180 ℃ corresponds to loss of MeOH molecules and DMF molecules. The second weight loss between 450 ℃ and 533 ℃ can be ascribed to loss of ligand and then the collapse of frameworks (cacld 66 %). For as-synthesized **NAT-MOF-2** (Figure S3b, red curve), the first weight loss of 5 % happened between 29 ℃ and 65 ℃ demonstrates loss of H_2O molecules adsorbed on surface of framework. The second weight loss of 18 % between 65 ℃ and 130 ℃ contributes to H_3O^+, coordinated H_2O molecules and part of guest DMF molecules. The third weight loss of 17 % belongs to loss of coordinated DMF molecules between 130 ℃ and 416 ℃. Final weight loss of 46 % between 416 ℃ and 530 ℃ refers to collapse of framework. Interestingly, both activated NAT-MOFs show effective guest molecules removal and have similar thermal stability with no decomposition at 413 ℃ and 434 ℃ until completely collapse at around 530 ℃.

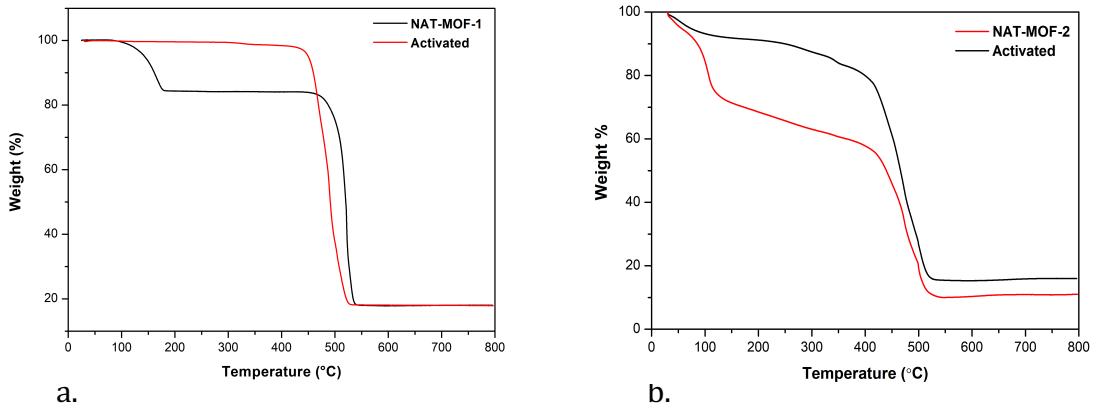

Figure S3. TGA curves of (a) **NAT-MOF-1** (b) and **NAT-MOF-2**

3.7 Gas adsorption experiments

As mentioned before, the N_2 and CO_2 gas adsorption measurements were performed on a Micromeritics ASAP 2020 (P/P_0 = 0-1.0). **NAT-MOF-1** was solvent exchanged with anhydrous ethanol which was changed every one hour for 72 h. **NAT-MOF-2** was solvent exchanged with anhydrous MeOH and the same changed the solvent every one hour for 3 days. Then, both **NAT-MOF-1** and **NAT-MOF-2** were dried under a dynamic vacuum at 85 ℃ for 24 hours and degas again at 85 ℃ on the instrument for 12 h before starting the adsorption and desorption tests. Figure S4 reveals pore width distribution of **NAT-MOF-1** and **NAT-MOF-2,** it is obvious to find that **NAT-MOF-1** has more mesopores than **NAT-MOF-2** which corresponds to higher BET than **NAT-MOF-2**. CO_2 / N_2 selectivity at 273 K of **NAT-MOF-2** was calculated via IAST theory to be 4.8 in general (Figure S5).

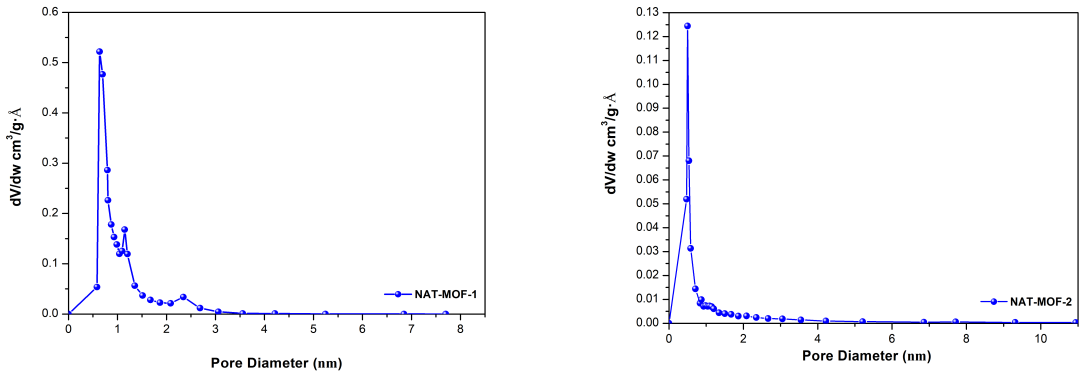

Figure S4. Pore width distributions of **NAT-MOF-1** and **NAT-MOF-2**

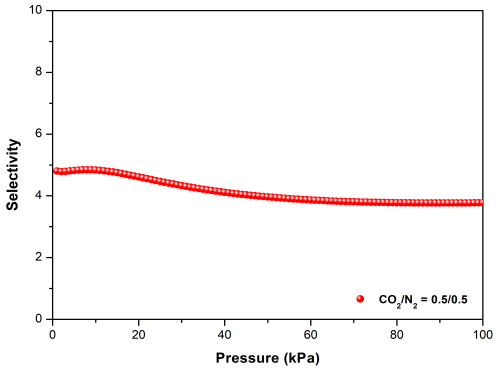

Figure S5. 273 K CO_2 /N_2 selectivity of **NAT-MOF-2**

3.8 NMR Spectra

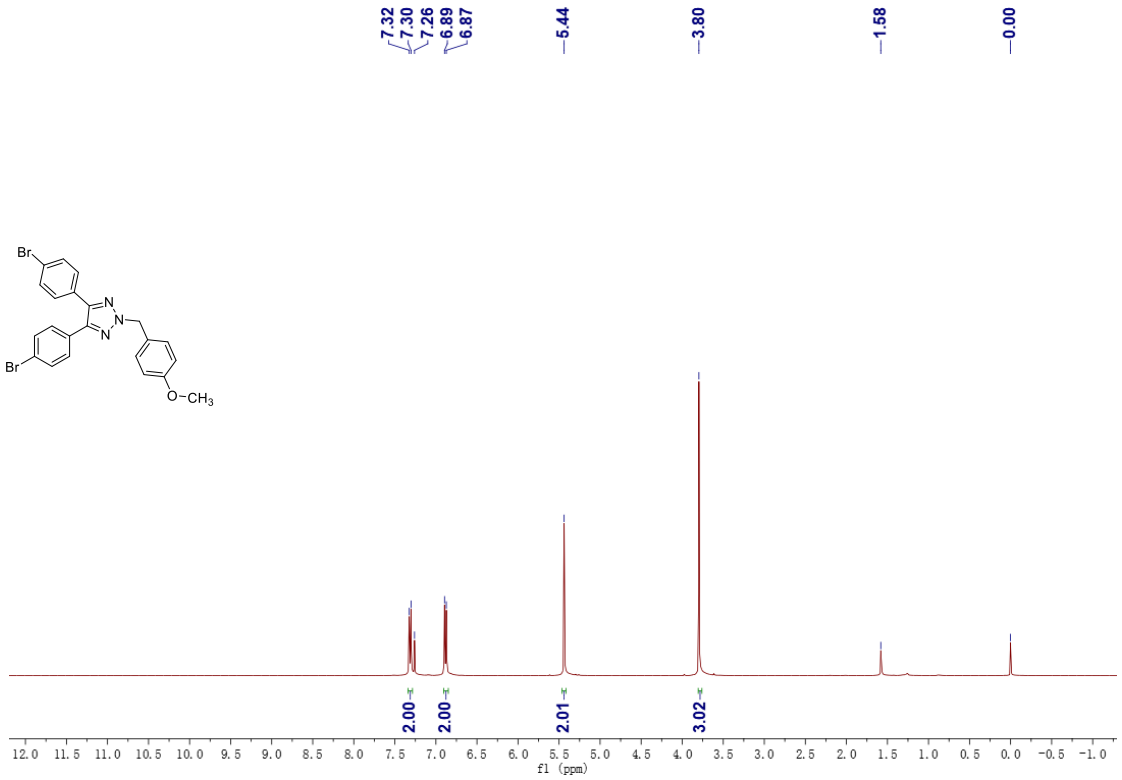

Figure S6. ^{1}H NMR spectrum of compound **1**.

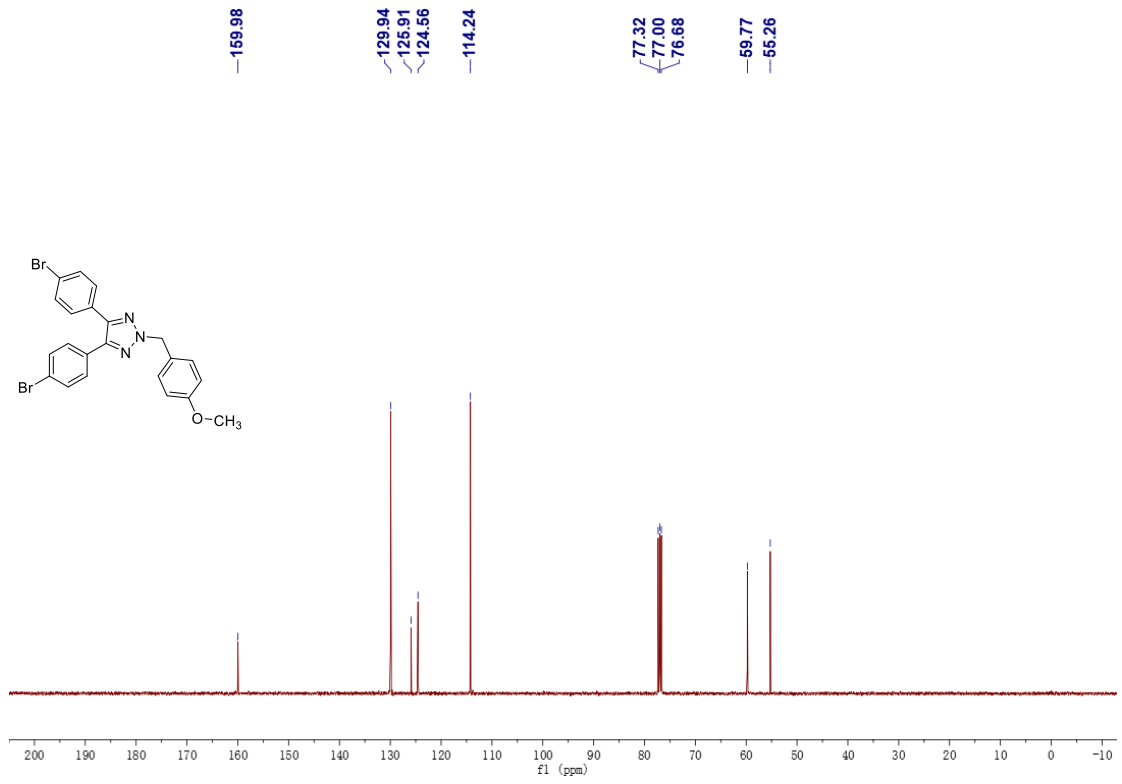

Figure S7. ^{13}C NMR spectrum of compound **1**.

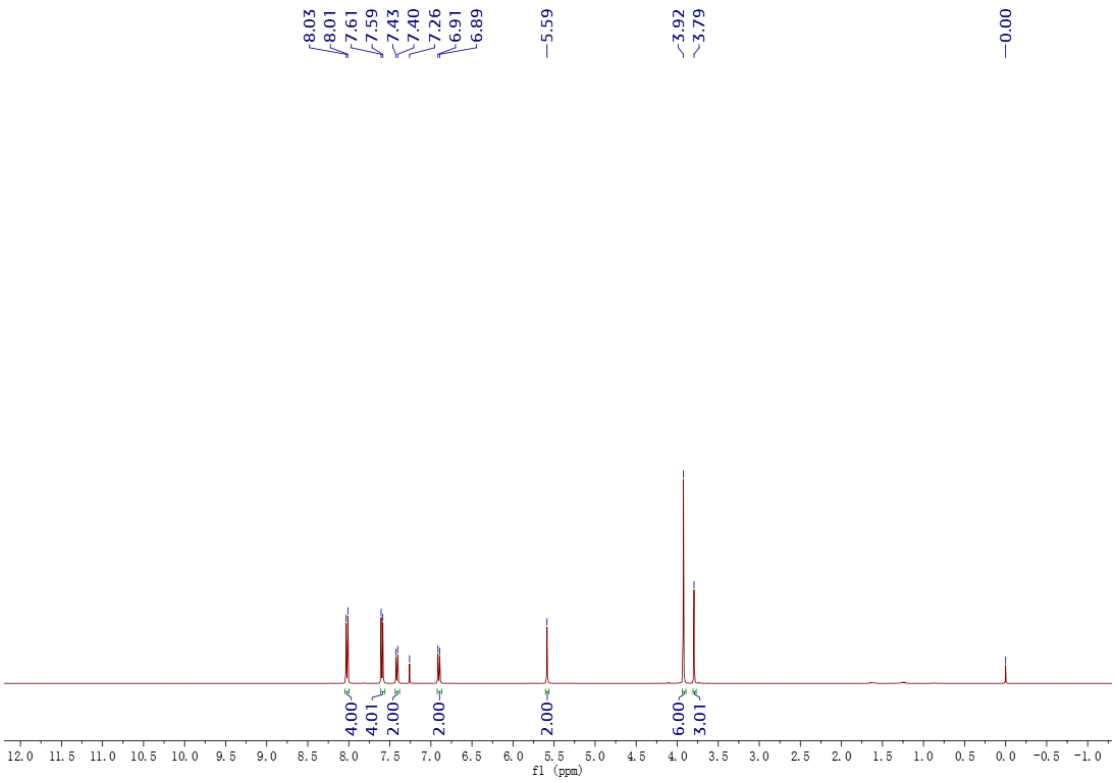

Figure S8. ^{1}H NMR spectrum of compound **2**.

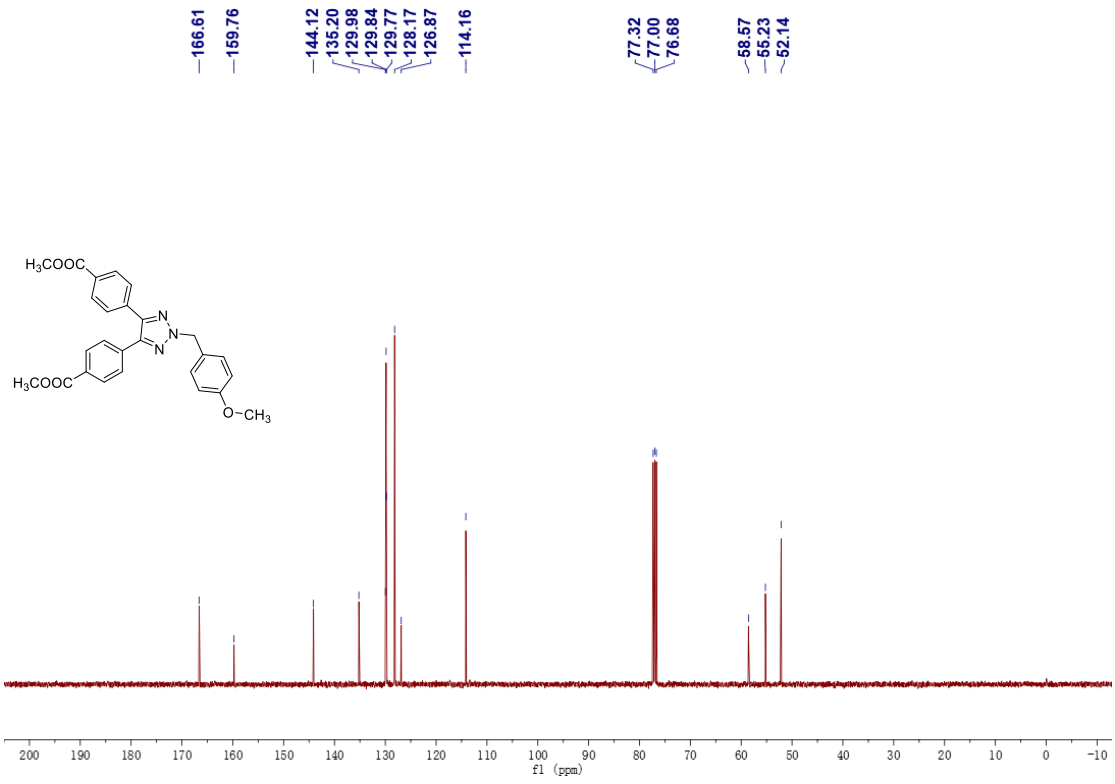

Figure S9. ^{13}C NMR spectrum of compound **2**.

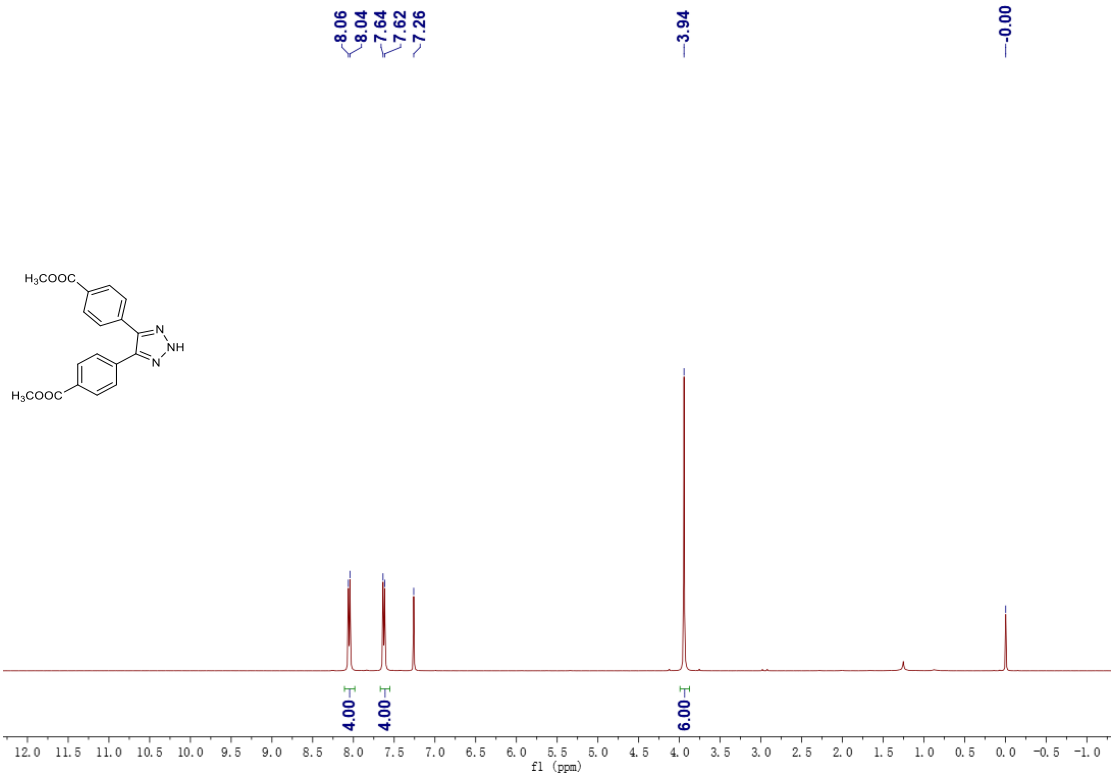

Figure S10. ^{1}H NMR spectrum of compound **3**.

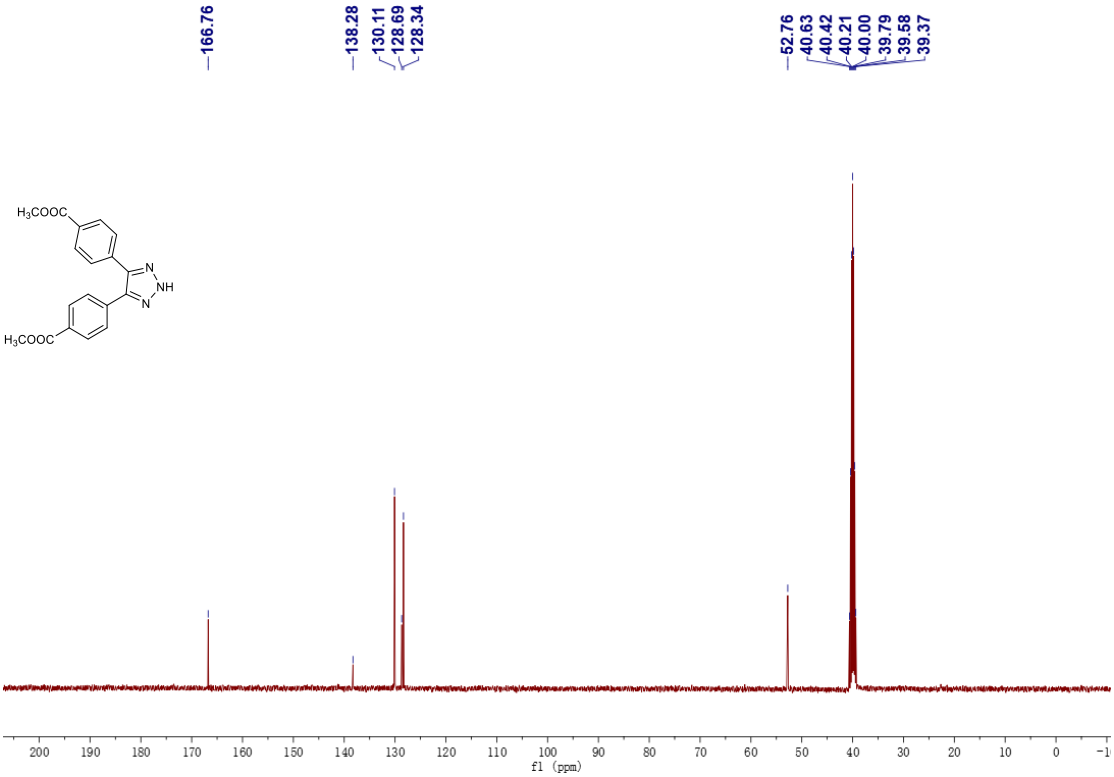

Figure S11. ^{13}C NMR spectrum of compound **3**.

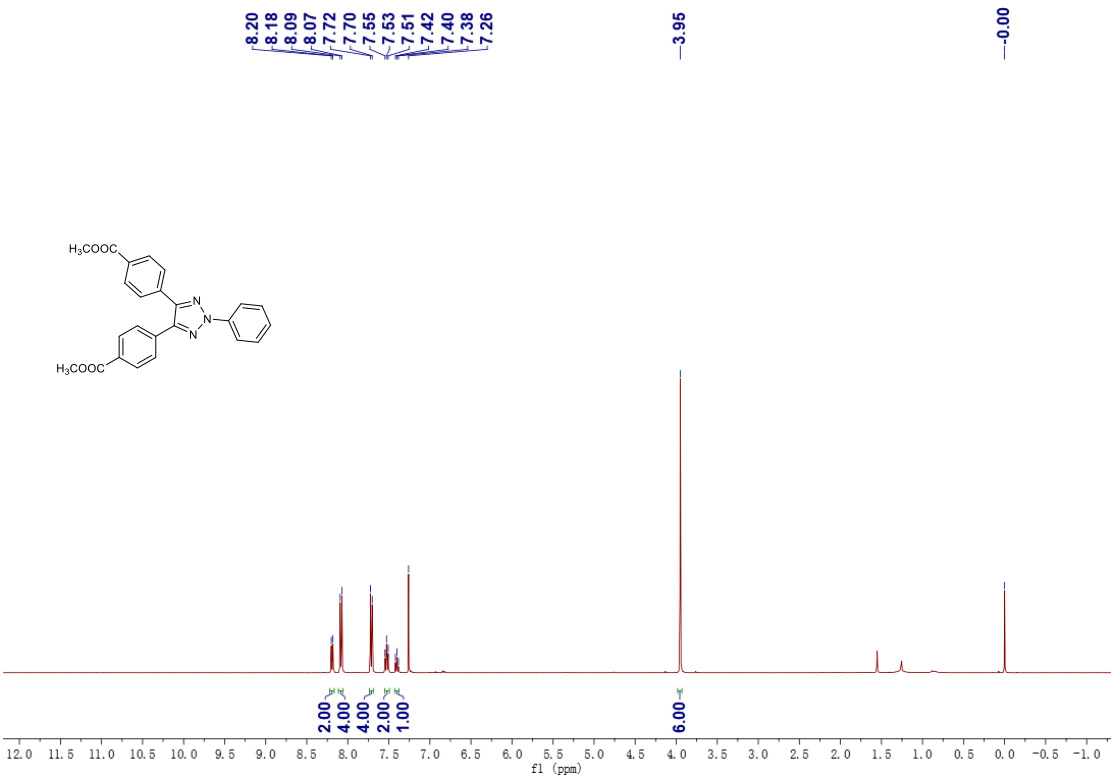

Figure S12. ^{1}H NMR spectrum of compound **4**.

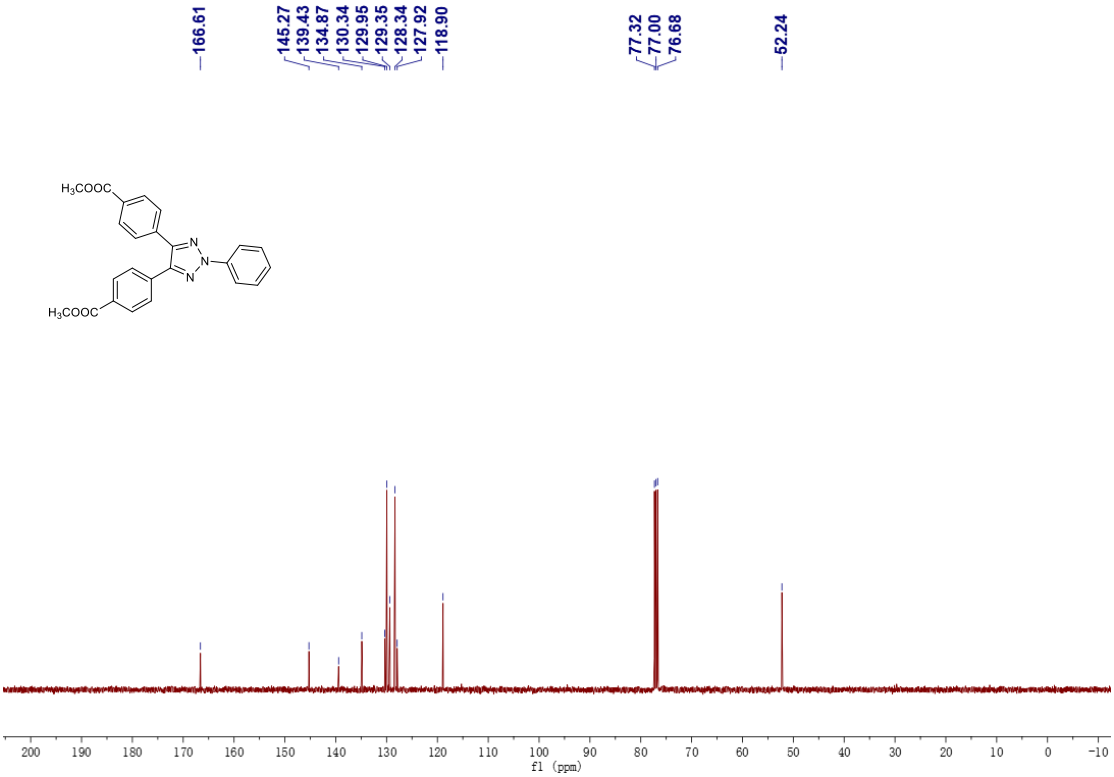

Figure S13. ^{13}C NMR spectrum of compound **4**.

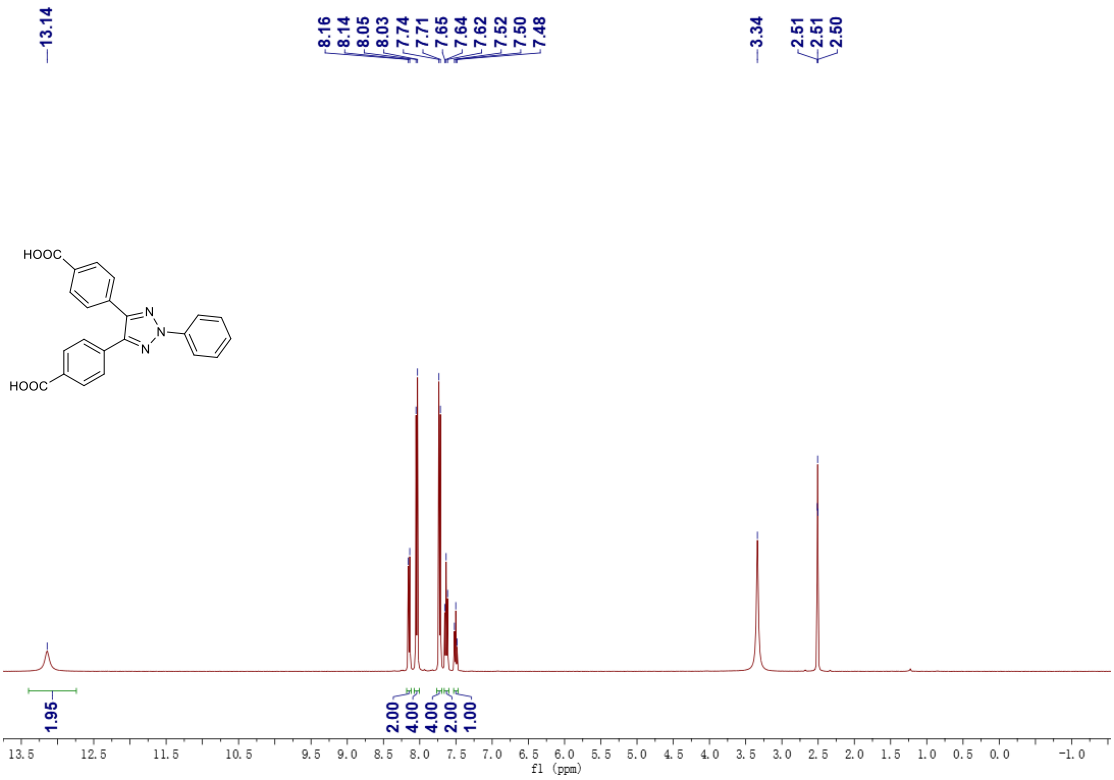

Figure S14. ^{1}H NMR spectrum of compound **L1**.

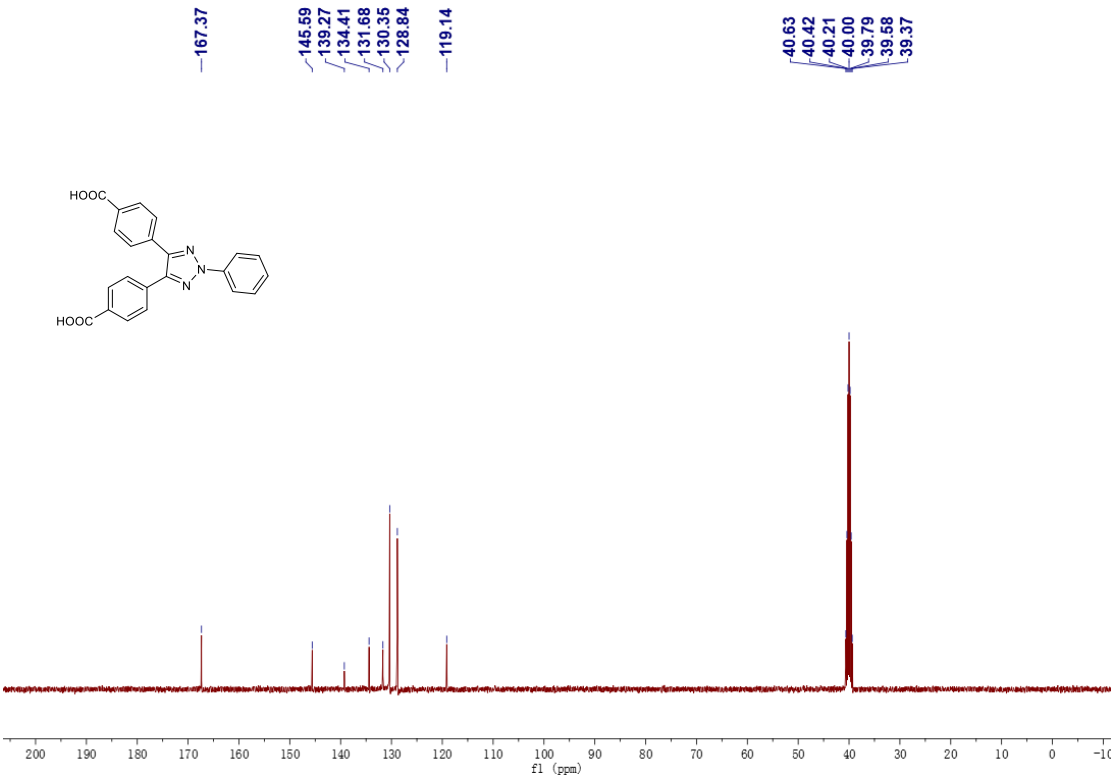

Figure S15. ^{13}C NMR spectrum of compound **L1**.

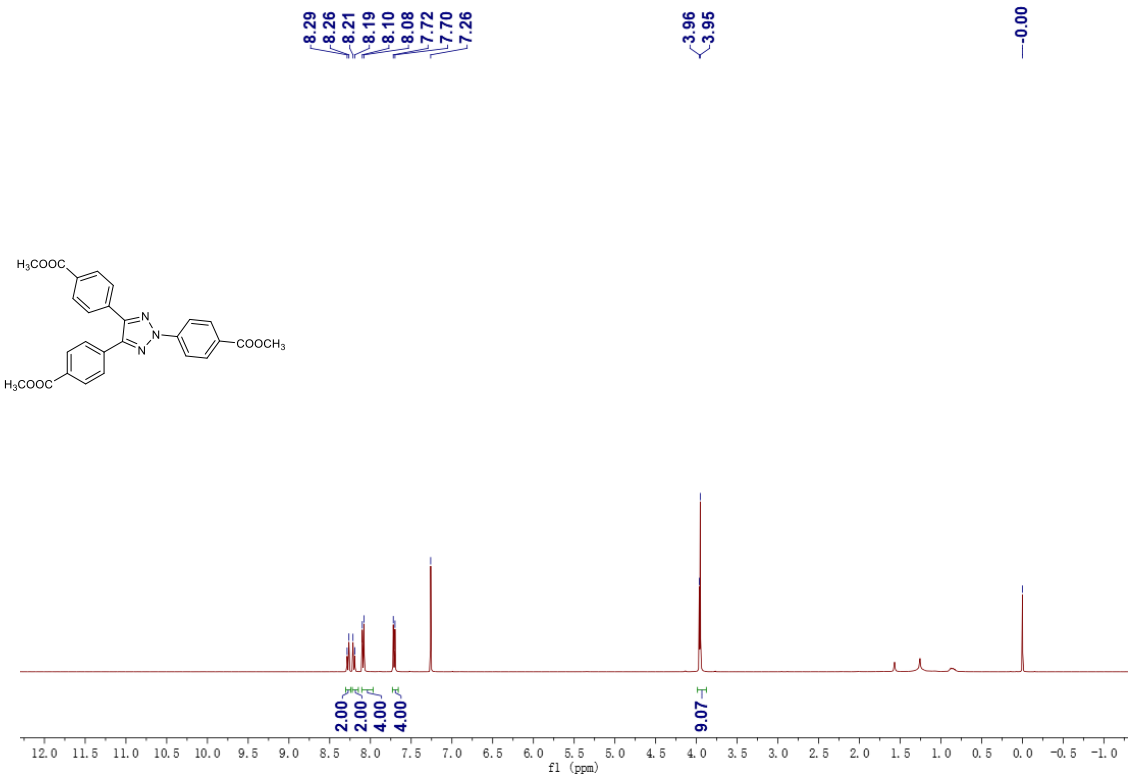

Figure S16. ^{1}H NMR spectrum of compound **5**.

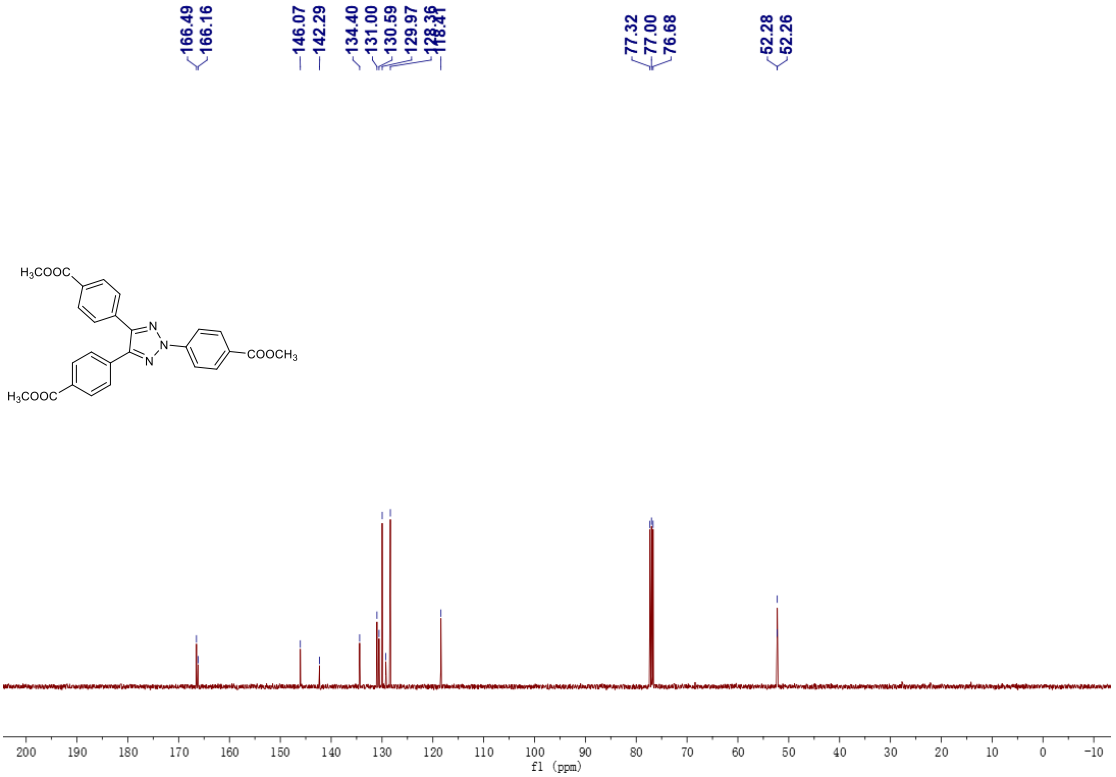

Figure S17. ^{13}C NMR spectrum of compound **5**.

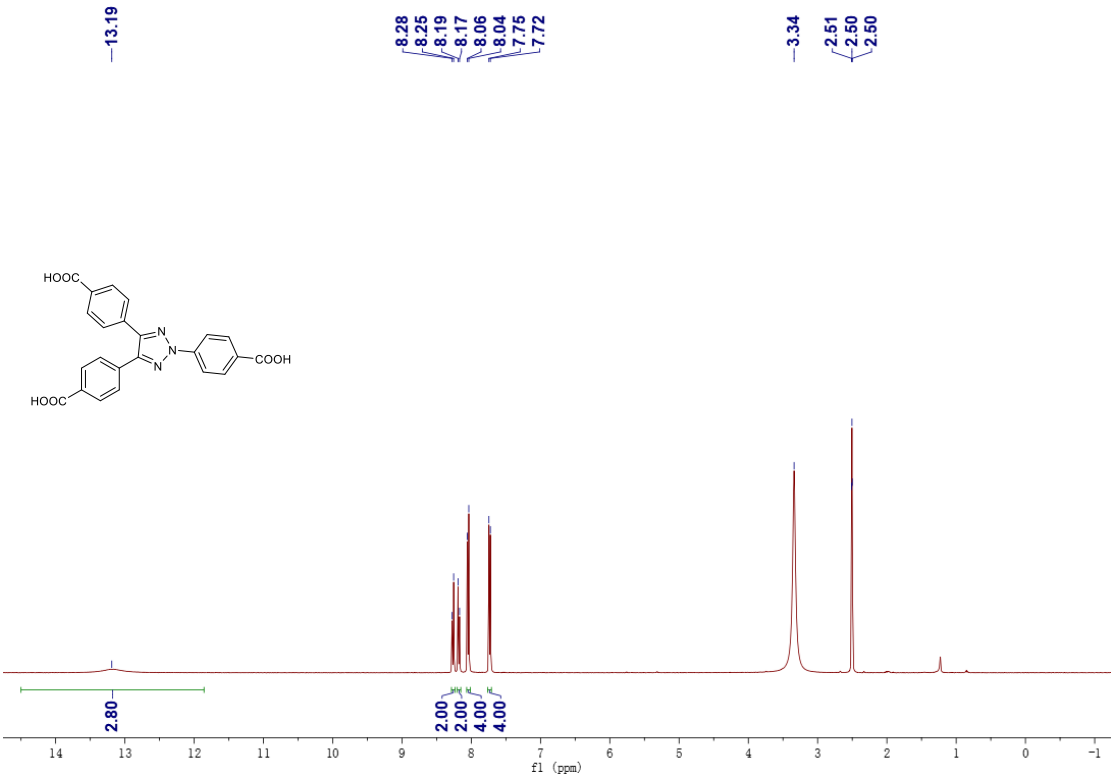

Figure S18. ^{1}H NMR spectrum of compound **L2**.

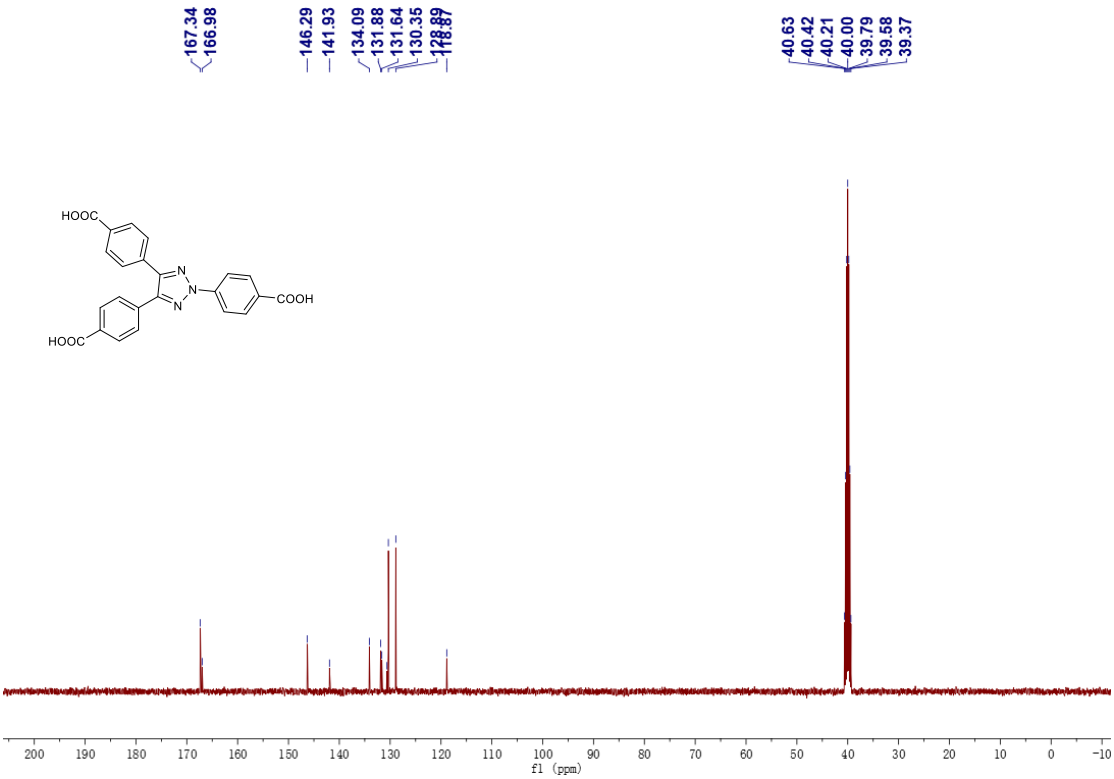

Figure S19. ^{13}C NMR spectrum of compound **L2**.